Inhibition by Water during Heterogeneous Brønsted Acid Catalysis by Three-Dimensional Crystalline Organic Salts

Alexander Gak,[1,2,3] Svetlana Kuznetsova,[1] Yulia Nelyubina,[1] Alexander A. Korlyukov,[1] Han Li,[4] Michael North,[4] Vladimir Zhereb,[5] Vlagimir Riazanov,[6] Alexander S. Peregudov,[1] Ekaterina Khakina,[1] Nikolai Lobanov,[7] Victor N. Khrustalev,[7,8] and Yuri N. Belokon[*1]

1) A. N. Nesmeyanov Institute of Organoelement Compounds, Russian Academy of Sciences, Vavilov Street 28, 119991 Moscow, Russian Federation; 2) Moscow State University, Faculty of Material Science, Leninskie Gory, 1/40, 119991 Moscow, Russian Federation; 3) National Research Nuclear University MEPhI, Institute of Nuclear Physics and Engineering, Kashirskoe shosse 31, 115409, Moscow, Russian Federation; 4) Green Chemistry Centre of Excellence, Department of Chemistry, University of York, Heslington, York, YO10 5DD, UK; 5) Siberian Federal University, School of Non-Ferrous Metals and Material Science, 95 Krasnoyarskiy Rabochiy pr., 660025 Krasnoyarsk, Russian Federation; 6) D. Mendeleev University of Chemical Technology of Russia, Miusskaya square 9, 125047 Moscow, Russian Federation; 7) Peoples' Friendship University of Russia (RUDN University), 6 Miklukho-Maklaya Street, Moscow 117198, Russian Federation; 8) N.D. Zelinsky Institute of Organic Chemistry, Russian Academy of Sciences, 47 Leninsky Prospect, Moscow 119991, Russian Federation.

*Email: yubel@ineos.ac.ru

KEYWORDS: Charge assisted hydrogen bonded frameworks; Brønsted acid catalyst; epoxide ring-opening; acetal formation; heterogeneous catalyst, water inhibition.

Abstract: A new, self-assembled and self-healing class of metal free, recyclable, heterogeneous Brønsted acid catalysts have been developed by the protonation of aniline derivatives (tetrakis-(4-aminophenyl)methane, leuco-crystal violet, benzidine and p-phenylenediamine) with aromatic sulfonic acids (tetrakis-(phenyl-4-sulfonic acid)methane, and 2,6-naphthalenedisulfonic acid). As a result, five three-dimensional crystalline organic salts (**F-1a**, **F-1b**, **F-1c**, **F-2** and **F-3**) were obtained, linked by hydrogen bonds and additionally stabilized by the opposite charges of the components. Frameworks **F-2** and **F-3** were prepared for the first time and characterized by elemental analysis, X-ray structural analysis (for **F-2**), thermogravimetry, SEM, and FTIR spectroscopy. The catalytic activities of crystalline organic salts **F-1-3** have been explored in industrially important epoxide ring-opening and acetal formation reactions. The presence of encapsulated water inside frameworks **F-1a** and **F-2** had an inhibitory effect on the performance of the catalysts. X-ray diffraction analysis of hydrated and dehydrated samples of **F-1a** and **F-2** indicated that water of crystallization served as a cross-linking agent diminishing the substrate induced "breathing" affinities of the frameworks.

Introduction

Homogeneous catalysis has been a huge success of the chemicals industry in the 20th century.[1-3] However, the recovery of homogeneous catalysts from the reaction medium at the end of reactions can be difficult. It seemed that this problem could be solved by immobilizing the catalysts on solid carriers. Nevertheless, despite numerous attempts to solve this problem, such catalysts are almost never used in industry.[4] The reason for this is the high price of such catalysts and their generally inferior catalytic performance as compared to homogeneous analogues. Inherent causes of the low activity of immobilized catalysts are the entropy enhanced self-association of catalytic centers on the polymeric supports, hindered substrate diffusion within the polymer network and a rapid loss of catalytic activity during the chemical process.[4]

In recent years, crystalline porous covalent organic frameworks (COFs)[5-9] and metalorganic frameworks (MOFs)[10-12] have been discovered and their applications broadly explored. The performance of their catalytic centers; either as part of the framework or as a separate entity embedded into the framework, is greatly enhanced as COFs and MOFs are free from the disadvantages inherent in conventional cross-linked polymeric systems.[9] This is due to COFs and MOFs having a regular porous structure so that the location of the key catalytic centers is set at fixed distances.[5-12] There are even cases where COF immobilized catalysts outperform their homogeneous analogs.[9] Unfortunately, such catalysts are expensive due to

Scheme 1. Synthesis of 3-D crystalline organic salts **F-1b**, **F-1c**, **F-2** and **F-3**.

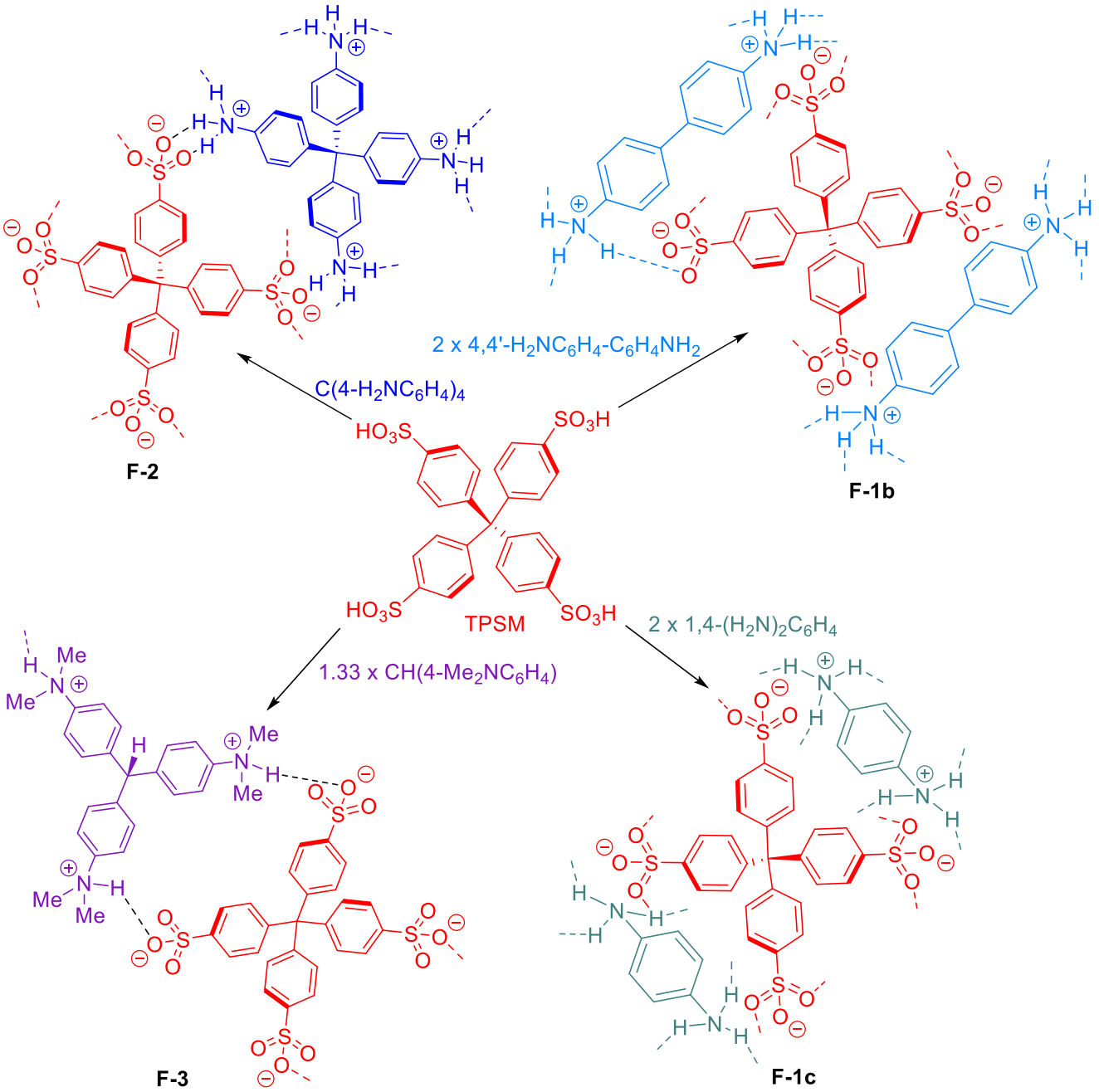

the price of the initial materials, and their use is impeded by the difficulty of their synthesis (especially COFs), and the low stability of MOFs, the decomposition of which is accompanied by the leaching of metal ions.[11]

Recently, a new type of framework based on non-covalent supramolecular interactions of components, containing several hydrogen bond donors and acceptors fixed in space by hydrogen bonds has been developed. These frameworks are called HOFs (hydrogen bonded frameworks)[13] and they can additionally be stabilized by electrostatic interactions.[14] The directional hydrogen bonds disfavor close packing of the tectons and thus, generate significant pore volumes within the crystals.[15-18] An additional advantage of HOFs is their self-healing properties, as the frameworks can easily self-reassemble after disassembly induced by an external stimuli.[16,17] This class of materials are displaying some promising advances in proton conductivity,[13,19] gas separation[20] and adsorption,[21] enzyme encapsulation[22] and even asymmetric synthesis.[23] The burgeoning field has been thoroughly assessed in two recent reviews.[24,25] However, the great potential of HOFs either heterogeneous catalysts in their own right, or as a platform for the attachment of catalytic centers is practically unexplored.[24,25]

Our work is directed towards creating a family of crystalline heterogeneous supramolecular acid catalysts based on ionic interactions of the components, supplemented by hydrogen bonds. They have the advantage of being

obtained by a simple one-step mixing of the components in water or organic solvents followed by separation of the formed precipitate. In previous work[26] we found that mixing together aqueous solutions of two equivalents of disodium 2,6-naphthalene-disulfonate (NDS) and one equivalent of the tetrahydrochloride of tetrakis(4-aminophenyl)methane (TAPM) at ambient temperature immediately produced **F-1a** as a white precipitate. The structure of the crystalline material was established by single crystal structure analysis and the framework was found to possess sufficient Brønsted acidity to promote epoxide ring-openings and a Diels-Alder reaction.[26] The study was a preliminary one, but indicated that even **F-1a**, which does not possess significant pores, was able to absorb substrates by rearrangement of the matrix via a process called stimuli induced breathing.[27] Still, it seemed self-evident that the porosity of a crystalline framework should be an important factor in making a heterogeneous catalyst much more efficient. In a recent publication, Teng Ben *et al.* described porous HOFs **F-1b** and **F-1c** (Scheme 1) and reported that the materials had the best proton conductivity values reported to date for porous materials.[19] The water of crystallization was responsible for this phenomena. As Brønsted acidity is a process of proton transfer from an acid to a base, it seemed highly likely that the combination of porosity and water content within their framework would be conducive to the frameworks acting as heterogeneous catalysts.

In this work we have prepared novel crystalline organic salts **F-2** and **F-3** (Scheme 1) and studied the catalytic activities of water saturated and dehydrated **F-1a**, **F-1b**, **F-1c**, **F-2** and **F-3** in the ring-opening reactions of styrene oxide by methanol. Contrary to our expectations the experiments revealed that the water served as an inhibitor of the catalytic activities of **F-1a** and **F-2**, both derived from the tetradentate tecton TAPM. The origin of this phenomena was traced to the water molecules inside the frameworks functioning as a cross linking agent and decreasing the flexibility of the matrix. In contrast, the catalytic activity of **F-1b**, **F-1c** and **F-3**, constructed from tetrakis(4-phenylsulfonic acid)methane hydrates (TPSM), were relatively insensitive to hydration due to the relatively minor cross-linking effect of water inside their matrices. Finally, a simple procedure for acetal formation, employing the frameworks as recoverable heterogeneous Brønsted acid catalysts has been developed.

Results and Discussion

Framework **F-1a** was prepared as we have previously described[26] and **F-1b,c** were synthesized according to the procedure reported by Teng Ben et al.[19] **F-2** was made by mixing a solution of TAPM in THF with an aqueous solution of TPSM and the resulting precipitate was filtered to give **F-2** (Scheme 1). Framework **F-3** was prepared as a precipitate when solutions of four equivalents of leuco-crystal violet (tris(4-dimethylaminophenyl)methane, LCV) in dichloromethane and three equivalents of TPSM in methanol were mixed.

Solid **F-2** was insoluble in organic solvents except for DMSO. A few days after complete dissolution of **F-2** in DMSO, crystals of **F-2** spontaneously appeared in the solution. X-ray diffraction analysis (Figure 1, CCDC2093978) showed that the unit cell belonging to a tetragonal space group ($P4/n$) and contains two TAPM cations, two TPSM anions and eight molecules of DMSO, so that only one

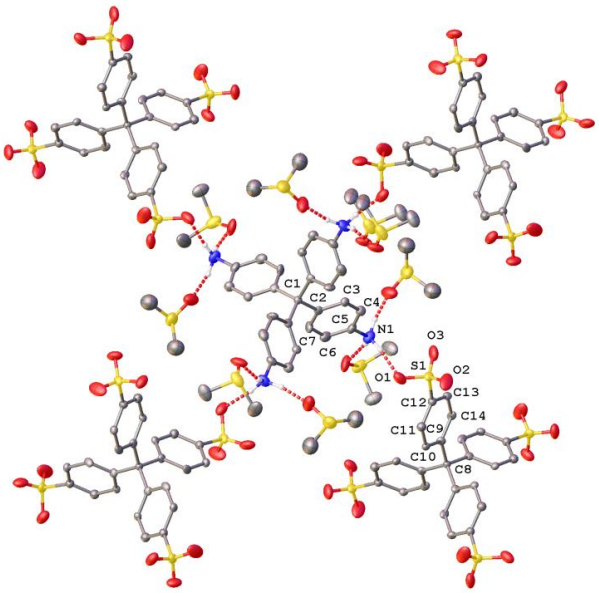

Figure 1. X-ray structure of a crystal of **F-2** grown from DMSO, illustrating the crystal environment around the cation and the hydrogen bonds it forms with anions/solvent molecules (shown as dashed lines). Hydrogen atoms (except those of ammonium groups) and the minor component of the disordered anion are omitted for clarity. Non-hydrogen atoms are shown as thermal ellipsoids at 30% probability level and only symmetry-independent atoms are labelled.

quarter of the ions and two solvent molecules are symmetry-independent. These species are held together by numerous hydrogen bonds that the ammonium groups of TAPM form with two DMSO molecules (N...O 2.67(2) and 2.716(18) Å, NHO 165.0(8) and 149.6(9)°) and with two oxygen atoms of the sulfonate group of the neighboring TPMS anions (N...O 2.96(3) and 3.00(3) Å, NHO 137.5(11) and 1363.7(10)°). The resulting hydrogen-bonded three-dimensional-framework contains small pores with the volume of the largest spherical void, calculated using the calcvoid routine implemented in Olex2,[28] being 11.5 Å^3.

Another batch of crystals of **F-2** was grown at the interface of carefully layered solutions of TAPM in THF and TPSM decahydrate in water. X-ray diffraction analysis of these crystals of **F-2** (Figure 2, CCDC2093979) showed it to be another tetragonal crystal phase, with space group $I4_1/a$. The composition is the same as in the DMSO-derived crystalline product, but with water as the lattice solvent instead of DMSO. The hydrogen bonding between the TAPM cation and the TPSM anion is also similar, although it involves only one oxygen atom of the sulfonate group (N...O 2.787(3) Å, NHO 163.58(17)°), and the two symmetry-independent water molecules (N...O 2.752(3) and 2.716(3) Å, NHO 160.22(17) and 159.43(18)°). However, the hydrogen-donor ability of the water molecules, which is lacking in DMSO, produces an extra set of hydrogen bonds that they

form with each other (O...O 2.825(3) Å, OHO 168.90(15)°) and with the TPMS anions (O...O 2.713(3)–2.812(3) Å, OHO 158.39(14)–176.15(15)°). The result is a much denser hydrogen-bonded three-dimensional-framework, with the volume of the largest spherical void being only 4.2 Å^3.

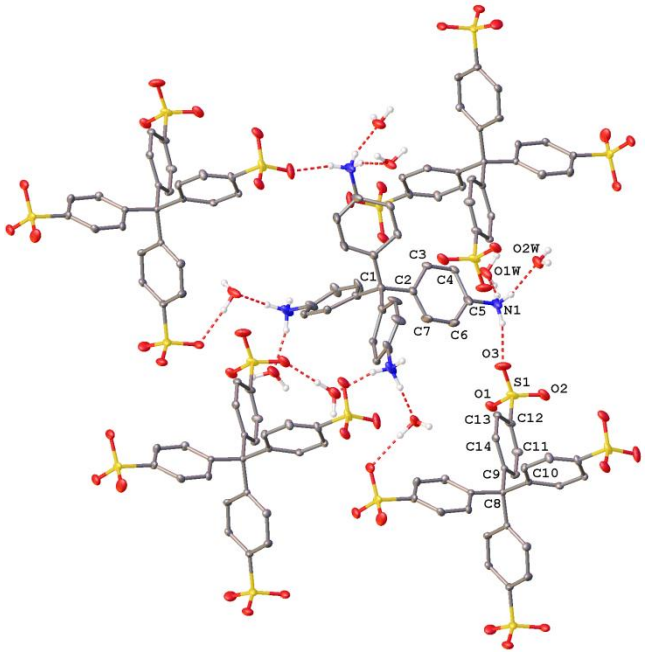

Figure 2. X-ray structure of a crystal of **F-2** grown from an aqueous solution of TPSM and a solution of TAPM in THF, illustrating the crystal environment of the cation and the hydrogen bonds it forms with anions/solvent molecules (shown as dashed lines). Hydrogen atoms (except those of ammonium groups) and the minor components of the disordered ions are omitted for clarity. Non-hydrogen atoms are shown as thermal ellipsoids at 30% probability level and only symmetry-independent atoms are labelled.

The powder X-ray diffraction (PXRD) pattern (Figure 3a) of the as-prepared crystalline samples of **F-2** corresponded to the same tetragonal phase found for the single crystals grown from water/THF solution. The size of the crystallites calculated from integral broadening was 65 nm. In contrast, a dried sample of **F-2** was lacking crystallinity, as its PXRD pattern showed only a wide maxima (Figure 3b). This behavior is different to the dehydration of **F-1a** reported earlier as **F-1a** retains its crystal structure with increasing void volumes even after complete dehydration.[26] The dehydrated sample of **F-2** (Figure 3b) recovers its crystallinity after being kept over water in a desiccator (Figure 3c). However, the sample remained amorphous if kept for the same time over methanol (Figure 3d).

Framework **F-3** was practically insoluble in various nonpolar organic solvents but was highly soluble (with dissociation of its components) in water and DMSO. This can be rationalized on the basis that it can only form one third of the hydrogen bonds that frameworks **F-1a-c** and **F-2** can form. In polar solvents, swelling of **F-3** occurred resulting in the formation of gels. As a result, it was not possible to grow crystals of **F-3** for X-ray diffraction analysis.

a)

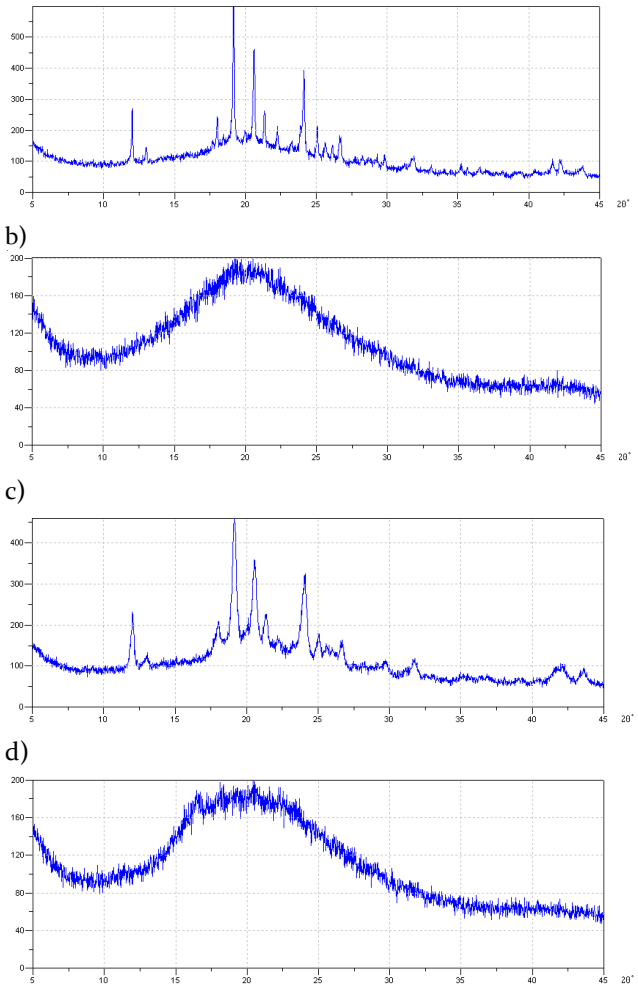

Figure 3. a) PXRD pattern of as-prepared crystalline **F-2**. b) PXRD pattern of **F-2** after being dried at 110 °C and 2 kPa for 0.5 hours. c) PXRD pattern of the dehydrated sample of **F-2** after being kept in a desiccator over water for 48 hours. d) PXRD pattern of the dehydrated sample of **F-2** after being kept in a desiccator over methanol for 48 hours.

The morphologies of samples of **F-2** and **F-3** were studied by scanning electron microscopy (SEM) (see supporting information). The morphologies of **F-1a-c** were reported previously.[19,26] The SEM images showed that the samples of **F-2** and **F-3** differed significantly. Framework **F-2** was composed of crystals of different forms, most likely originating from different kinetics associated with each crystal formation. Local X-ray spectral analysis (Figures S1-S4) showed that the chemical elements were distributed evenly on the sample surface, which supports its single phase structure. The sample of **F-3** consisted of almost amorphous or badly crystalline particles, with sizes of 60 to ~350 μm. The presence of microcracks on the surface of the particles is due to water removal from the near surface layers which indicates a multilayer arrangement of the samples. Local X-ray spectral analysis (Figure S6) again showed that the chemical elements were distributed evenly on the sample surface supporting its single phase structure.

Thermogravimetric analysis (TGA) data for samples of **F-2** and **F-3** are shown in Figure 4a,b. Framework **F-2**

underwent a 13% weight loss between room temperature and 200°C with the maximum rate of weight loss occurring at 117 °C. FTIR analysis of the evolved gases showed that this weight loss was due to removal of water of crystallization

a)

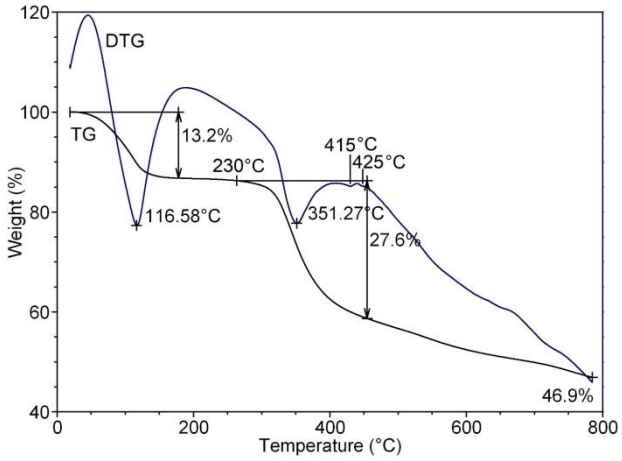

b)

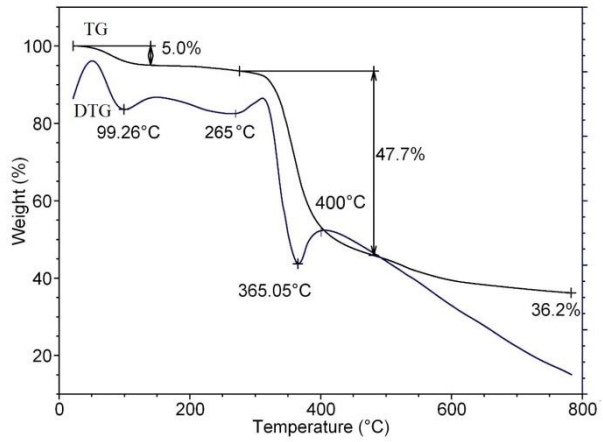

Figure 4. TGA analysis of samples of a) **F-2** and b) **F-3**.

from the sample. Further weight loss took place from 230–400 °C with a maximum rate at 350 °C and was the outcome of aniline loss. Further degradation was observed at 400–480 °C and was a consequence of sulfur dioxide and ammonia loss. Framework **F-3** initially lost 5% of its weight around 100 °C with the maximum rate of loss at 99 °C (Figure 4b). This loss can be attributed to the removal of water of crystallization from the sample. A further 48% weight loss took place from 265–400 °C as a result of toluidine and ammonia loss. Further degradation with methane and benzene evolved was observed around 500 °C.

All the framework samples absorbed water and the capacity to do so was not related to the porosity of the samples (Table 1). For example, **F-1c** has the highest porosity in the series, as indicated by its surface area being an order of magnitude higher than any other framework. However, the amount of water it could absorb was the second lowest in the series. The structure of **F-1b** shows all the ammonium groups of the 4,4'-diaminobiphenyl (PDP) units connected by three hydrogen bonds to the sulfonate groups of three neighboring TPSM tetra-anions. Water molecules do not bridge the two salt components, but are hydrogen bonded to the neighboring sulfonate groups.[19] In **F-1c** each ammonium group of para-phenylenediamine (PPD) formed two hydrogen bonds with two sulfonate anions of two neighboring TPSM tetra-anions and the third ammonium proton was connected with the sulfonate of a third TPSM molecule via a bridge formed by two water molecules.[19] On the other hand, framework **F-2** has its TAPM ammonium groups connected via two water molecule bridges with two neighboring sulfonate groups of two different tetra-anions of TPSM and only one hydrogen bond was formed with the sulfonate moiety of a third TPSM (Figure 2). Thus, water evidently plays an important role in stabilizing the salts when the direct hydrogen bonding of ammonium and sulfonate groups becomes impossible. This occurs, most likely, from crystal packing difficulties in **F-2**, **F-1a** and **F-1c**. In any case, water provides hydrogen bonds to the anions and its lone pairs to the ammonium groups. Consistent with this analysis, dehydrated samples of **F-2** become destabilized and slowly decompose with the formation of carbocations and aniline, as shown in Scheme 2. Dehydration of **F-2** does not lead to the formation of large pores as judged by the

BET surface area (Table 1). However, pores do form if hydrogen bond acceptors such as DMSO come into the

Scheme 2. **F-2** decomposition pathway.

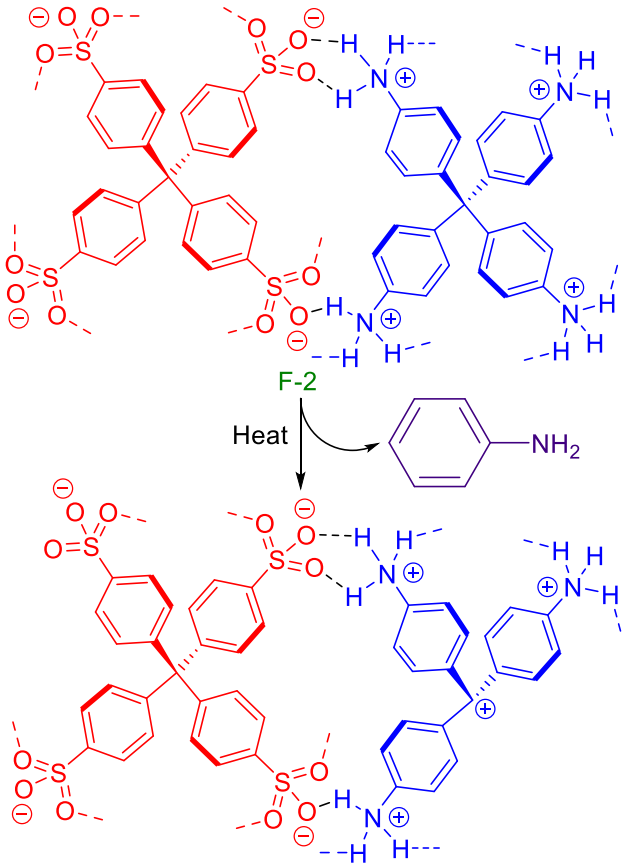

Table 1. The water absorption capacity of the crystalline organic salts

Salt	BET Surface area ($m^2 g^{-1}$)	Amount of H_2O in the saturated salt (mass %)[a]	Number of H_2O molecules in the saturated salt [b]	Amount of H_2O in the dehydrated salt (mass %)[c]	Number of H_2O molecules in the salt after dehydration[b]
F-1a[d]	2.6	7.5	4.3	0.5	0.3
F-1b[e]	12	13.8	9.0	0.8	0.5
F-1c[e]	129	12.0	6.4	0.8	0.4
F-2	5.5	17.1	11.7	0.6	0.4
F-3	n.d.	24.5	20.7	0.6	0.3

[a]Samples were kept in a desiccator under a water saturated atmosphere for 24–48 h. [b]Calculated per TAPM or TPSM unit. [c]Samples were kept in vacuo at 110 °C for 3 h and the water content was estimated by Fisher titration. [d]Taken from Ref.26. [e]Taken from Ref.19.

structure (Figure 1) with voids, occurring near the sulfonate and ammonium groups.

Framework **F-3** had four molecules of leuco-crystal violet (LCV) protonated by three molecules of TPSM (Scheme 1). Only one hydrogen bond can be formed between each dimethylammonium group of LCV and each sulfonate group of TPSM . As a result, the rigidity of the framework was greatly diminished as compared to **F-1a-c** and **F-2**, and the solvating water is easily absorbed inside the framework (Table 1) with accompanying swelling of the matrix.

Expectedly, **F-3** was the most soluble (with dissociation of its components) amongst all the frameworks in both methanol and a methanol/dichloromethane mixture (Table 2). Salts **F-1a** and **F-2**, both based on TAPM, were less soluble in methanol than **F-1b** and **F-1c** derived from TPSM. The solubility of the frameworks was very low in the methanol/dichloromethane mixture but the solubility of **F-1b** and **F-1c** fell most drastically.

The opening of styrene oxide with methanol was chosen as a model reaction to explore the catalytic properties of the crystalline organic salts (Scheme 3). The reactions were conducted in a methanol/dichloromethane solution (20 equivalents of methanol relative to styrene oxide) at

Table 2. The solubility (with component dissociation) of the frameworks (mol/l)[a]

Salt	MeOH (mol l^{-1} x 10^5)	MeOH/CH_2Cl_2[b] (mol l^{-1} x 10^5)	THF (mol l^{-1} x 10^5)
F-1a	1.5	0.1	<0.01
F-1b	176	<0.01	<0.01
F-1c	118	<0.01	<0.01
F-2	2.5	0.1	<0.01
F-3	816	5.2	n.d.

[a]The solution was completely saturated with a salt, filtered and the amount of the dissolved framework was determined by ^{1}H NMR spectroscopy with a standard solution of p-dinitrobenzene. [b]The solvent was composed of 3 ml of MeOH and 20 ml of CH_2Cl_2.

Scheme 3. Reaction of styrene oxide with methanol catalyzed by crystalline organic salts.

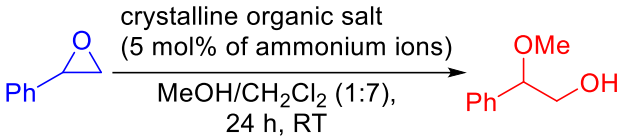

room temperature, conditions under which the salts were practically insoluble (Table 2). The reaction mixtures were mechanically stirred at a speed greater than 700 rpm to nullify the effect of stirring on the progress of the reaction as previously determined.[26] After the required reaction time, the reaction mixture was filtered, evaporated and analyzed by ^{1}H NMR spectroscopy.

The filtrates of frameworks **F-1a**, **F-1b**, **F-1c**, and **F-2** dispersed in methanol/dichloromethane were not catalytically active which proved that catalysis by the salts was heterogeneous in nature. The filtrate of salt **F-3** did produce 2-methoxy-2-phenylethanol in 3% yield, but this was insignificant compared to the 85% yield obtained using the unfiltered **F-3** dispersion (Figure 5). The salt (TSA) formed from para-toluenesulfonic acid and aniline was chosen as a benchmark homogeneous catalyst for the reaction. Reactions catalyzed by TSA were conducted in deuterated methanol/deuterated dichloromethane and monitored by ^{1}H NMR spectroscopy.

As Figure 5a,b illustrates, both **F-1a** and **F-2** derived from TAPM were catalytically active, but in both cases significant induction periods were observed when using water saturated catalyst samples. For **F-1a**, the induction period greatly diminished and for **F-2** it totally disappeared if the samples were previously dehydrated. Notably, dehydrated **F-2** had the same catalytic activity as the homogeneous TSA catalyst. As shown earlier, **F-1a** increases its internal voids on dehydration[26] and the same was true for **F-2** (Figures 1 and 2). Thus, removal of the water bridges which function as cross-linking agents inside the frameworks, made the matrices less rigid and more susceptible to substrate induced "breathing". This analysis was supported by an experiment in which water saturated **F-1a** was exposed to a solution of styrene oxide in dichloromethane for 20 hours followed by methanol

a) b)

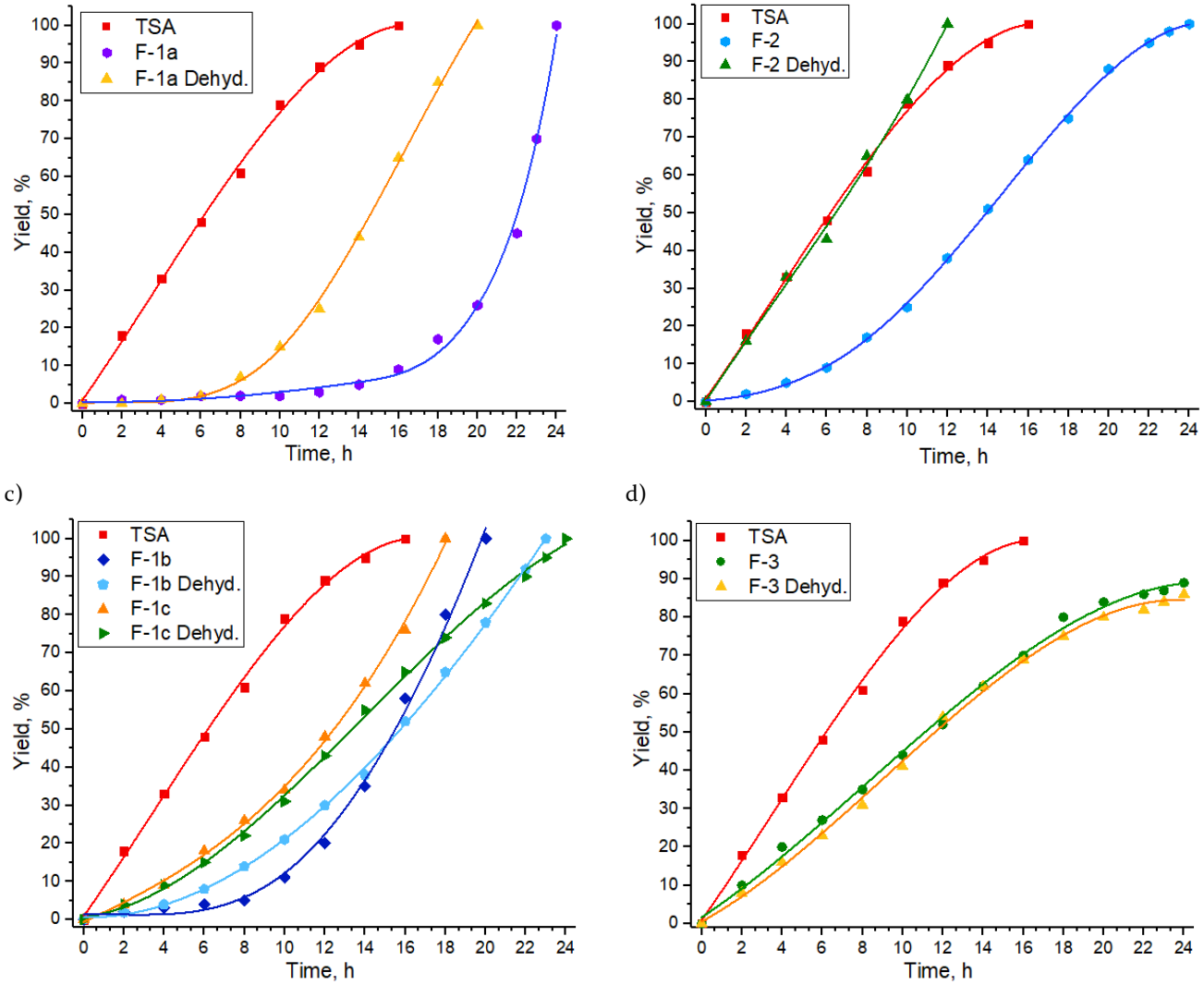

Figure 5. Styrene oxide ring opening with MeOH in CH_2Cl_2 at room temperature promoted by dehydrated and water saturated organic salts. a) **F-1a**, b) **F-2**, c) **F-1b** and **F-1c**, d) **F-3**. Reaction catalyzed by homogeneous TSA (red line) is included in each graph for comparison. MeOH (1.5 ml, 36.6 mmol), CH_2Cl_2 (10 ml), as obtained organic salt (9.61 x 10^{-5} mol of ammonium groups).

addition. After an additional six hours, the yield of 2-methoxy-2-phenylethanol was 20-30% rather than the 2% observed without the pretreatment. No changes were detected in the ^{1}H NMR spectrum of recovered **F-1a**. Therefore, reaction of styrene oxide with the intralattice water may explain the styrene oxide exposure promoting effect. This was supported by reaction of a water enriched sample of **F-2** with one equivalent of styrene oxide based on the expected amount of water in the framework. After 96 hours in dichloromethane at a room temperature, the filtrate contained 25% of 2-hydroxy-2-phenylethanol, as determined by ^{1}H NMR analysis.

Another feature of the catalysis by **F-1a** and **F-2** was the form of the reaction curves after the induction period was over. These indicated that the rate limiting aspect of the reactions was not the chemical reaction between the epoxide and methanol. The homogeneous TSA catalyst exhibited the same type of zero order kinetics, so diffusion of the reagents to acidic centers within the frameworks cannot be the rate determining step. The kinetics could be explained by assuming that styrene oxide molecules form hydrogen bonded complexes with the ammonium groups of **F-2** (or other frameworks or TSA) similar to that of DMSO as shown in Figure 1. Styrene oxide would saturate the acidic ammonium centers in a rapid pre-equilibrium, then reaction of the activated styrene oxide with methanol would be rate limiting and the rate of the reaction would be depend only on the concentration of ammonium centers and not on the substrate concentrations, resulting in zero order kinetics. Framework, **F-2** could be recycled five times without any deterioration of its catalytic properties provided that the reactions and isolation of **F-2** were carried out under argon to prevent its rehydration by atmospheric moisture.

The catalytic activity of **F-1b** was only slightly dependent on the dehydration of the sample (Figure 5c) as the water inside the matrix was not involved in the bonding of the salt components[19] and did not serve as a cross-linking agent. **F-1c** has slightly higher catalytic activity than **F-1b** (Figure 5c), but the difference is small compared to the difference in activity between **F-1a** and **F-2** (Figure 5a,b). The catalytic activity of **F-3** was independent of dehydration

(Figure 5d), as the components of the salt could be united by only one hydrogen bond and water could not serve as a cross-linking agent.

Acetal formation was also promoted by crystalline organic salts **F-1a** and **F-2** as shown in Scheme 4. Thus, reaction of 1-formylnaphthalene with methanol in a mixture of methanol and dichloromethane (ten equivalents of methanol relative to the aldehyde) gave the corresponding dimethyl acetal. The reversible reaction reached equilibrium, giving 65% of the acetal. The rates of reaction were followed by UV/Vis spectroscopy at 314 nm and 280 nm. Under the reaction conditions, water saturated crystalline organic salts were again inferior to the dehydrated samples of the frameworks (Figure 6). For this reaction, the performance of the homogeneous catalyst TSA was much better than that of **F-2** (assessed by ^{1}H NMR spectroscopy, in 7:1 CD_2Cl_2:CD_3OD). The homogeneous catalyst produced 59% of acetal after 5 minutes and 61% after 15 minutes. For catalysis by dehydrated **F-2**, these levels of conversion could only be achieved after 300 minutes (Figure 6). This drastic change in the relative catalytic activities of **F-2** and TSA in epoxide ring opening and acetal formation reactions could be partly attributed to the formation of water in case of acetal formation. This has little or no influence on the homogeneous catalyst, but inhibits the heterogeneous catalysts by the cross-linking effect as discussed above.

Scheme 4. Acetal formation promoted by organic salts.

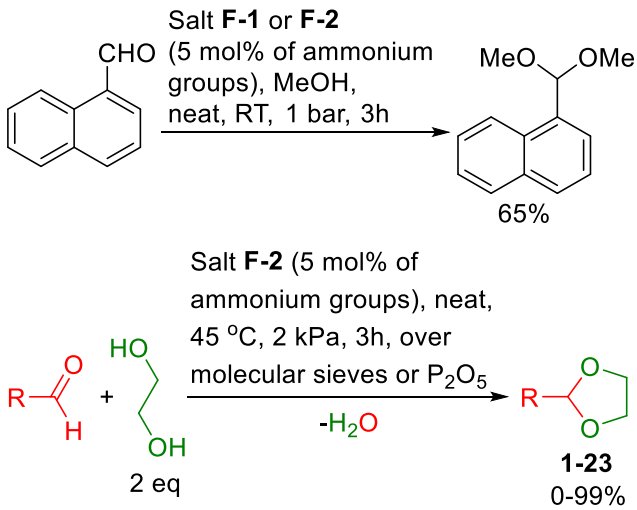

A general protocol for acetal formation was elaborated, employing **F-2** as the most efficient catalyst (Figure 6) and ethylene glycol as the alcohol component to increase the stability of the acetal. To shift the reaction equilibrium, water was removed by conducting the reaction under vacuum at 45 °C with the reaction vessel connected to a separate vessel, containing either phosphorus pentoxide or molecular sieves (Figure S19). The product of the reaction was extracted with toluene and **F-2** could be easily recovered by adding acetonitrile or THF and sonicating the mixture. Insoluble crystalline organic salt **F-2** was separated and dried at 45 °C. The recovered catalyst could be reused up to five times without any deterioration of its catalytic activity.

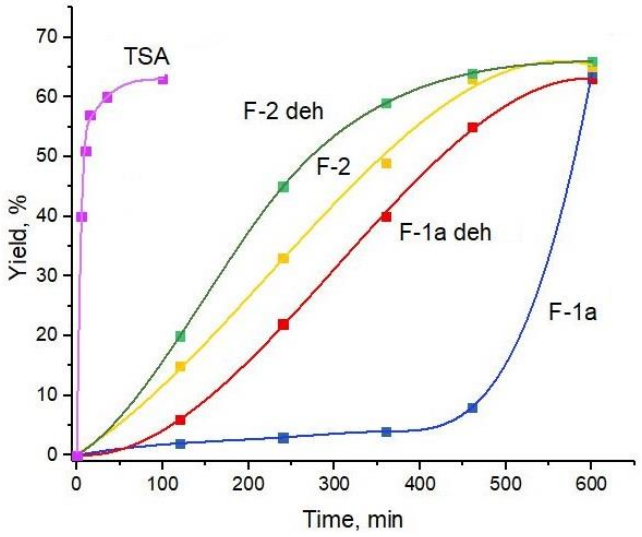

Figure 6. Reaction of 1-formylnaphthalene (1.83 mmol) with MeOH (1.5 ml) in a mixture of CH_2Cl_2:MeOH (7:1 by volume) promoted by TSA or dehydrated or water saturated **F-1a** and **F-2** (crystalline organic salt amounts were determined so as to provide 5 mol% of ammonium ions).

The results of these experiments are summarized in Table 3. A broad range of aldehydes could be converted into acetals with chemical yields up to 99% using the procedure. Aldehydes containing basic pyrrole or pyridine units were not substrates as they blocked the acidic, catalytic centers within **F-2**. 3-tert-Butylsalicylaldehyde and 9-formylphenanracene were also unreactive, probably for steric reasons.

Conclusions

Modularly prepared crystalline organic salts based on derivatives of tetrakis-(4-aminophenyl)methane (TAPM) and/or tetrakis-(phenyl-4-sulfonic acid)methane (TPSM), were found to be efficient and recoverable heterogeneous Brønsted acids, catalyzing both epoxide ring-opening and acetal formation. The catalytic efficiencies of the salts were not directly connected to their BET surface area. For the salts derived from TAPM (**F-1a** and **F-2**) the capacity to undergo substrate induced rearrangement (breathing) of the frameworks was the decisive factor in determining their catalytic activities. Water of crystallization formed bridges between the anions and cations thus stabilizing the frameworks and making the substrate induced breathing more difficult. As a result, the presence of water had an inhibitory effect on catalytic activity of **F-1a** and **F-2**. The catalytic efficiencies of the other crystalline organic salts, **F-1b**, **F-1c**, and **F-3**, were not affected by their hydration state, as water bridging between the anions and cations was either absent or insignificant. An efficient protocol for acetal formation promoted by the crystalline organic salts has been elaborated.

Table 3. Synthesis of acetals 1–23[a]

Aldehyde	Product	Time (h)	Yield (%)

PhCHO	**1**	3	97
Furan-2-CHO	**2**	3	95
Thiophene-2-CHO	**3**	9	93
4-MePyrrole-2-CHO	**4**	6	0
2-ClC_6H_4CHO	**5**	3	96
4-$Me_2CHC_6H_4CHO$	**6**	13	97
3-FC_6H_4CHO	**7**	3	99
2,3-$F_2C_6H_3CHO$	**8**	3	99
3,5-$F_2C_6H_3CHO$	**9**	3	98
2-F-4,5-$(MeO)_2C_6H_2CHO$	**10**	9	88
1-Formylnaphthalene	**11**	3	98
9-Formylanthracene	**12**	3	0
2-O_2N-4,5-$(OCH_2O)C_6H_2CHO$	**13**	9	99
2-$O_2NC_6H_4CHO$	**14**	3	87
3-$O_2NC_6H_4CHO$	**15**	3	99
$PhCH_2CH_2CHO$	**16**	3	99
PhCH=CHCHO	**17**	13	89
3-^{t}Bu-2-HOC_6H_3CHO	**18**	3	trace
2,3-Me_2-4-$MeOC_6H_2CHO$	**19**	9	85
3-$MeOC_6H_4CHO$	**20**	13	98
4-$MeOC_6H_4CHO$	**21**	13	86
Pyridine-3-CHO	**22**	3	0
Pyridine-2-CHO	**23**	3	trace

a Reaction conditions: Aldehyde (1.83 mmol), ethylene glycol (2 eq.), 45 °C, 2 kPa, amount of **F-2** determined so as to provide 5 mol% of ammonium groups.

ASSOCIATED CONTENT

Supporting Information. Details of experimental procedures, crystallography and instrumentation, copies of NMR and EDX spectra and SEM images. This material is available free of charge via the Internet at http://pubs.acs.org.

AUTHOR INFORMATION

Corresponding Author

*yubel@ineos.ac.ru

Author Contributions

The manuscript was written through contributions of all authors. All authors have given approval to the final version of the manuscript and all co-authors contributed equally.

ACKNOWLEDGMENT

X-ray diffraction data were collected with the financial support from the Ministry of Science and Higher Education of the Russian Federation using the equipment of Center for molecular composition studies of INEOS RAS and the RUDN University Strategic Academic Leadership Program.

REFERENCES

1. Busacca, C. A.; Fandrick, D. R.; Song, J. J.; Senanayake, C. H. The Growing Impact of Catalysis in the Pharmaceutical Industry. *Adv. Synth. Catal.* **2011**, *353*, 1825–1864.

2. Schlogl, R. Catalysis 4.0. *ChemCatChem* **2017**, *9*, 533–541.

3. Hayler, J. D.; Leahy, D. K.; Simmons, E. M. A. Pharmaceutical Industry Perspective on Sustainable Metal Catalysis. *Organometallics* **2019**, *38*, 36–46.

4. Jones, C. W. On the Stability and Recyclability of Supported Metal-Ligand Complex Catalysts: Myths, Misconceptions and Critical Research Needs. *Top. Catal.* **2010**, *53*, 942–952.

5. Zhang, G.; Hua, B.; Dey, A.; Ghosh, M.; Basem, A.; Moosa, B. A.; Niveen, M.; Khashab, N. M. Intrinsically Porous Molecular Materials (IPMs) for Natural Gas and Benzene Derivatives Separations. *Acc. Chem. Res.* **2021**, *54*, 155–168.

6. Gui, B.; Lin, G.; Huimin, D.; Gao, C.; Mal, A.; Wang, C. Three-Dimensional Covalent Organic Frameworks: From Topology Design to Applications. *Acc. Chem. Res.* **2020**, *53*, 2225–2234.

7. Lyle, S. J.; Waller, P. J.; Yaghi, O. M. Covalent Organic Frameworks: Organic Chemistry Extended into Two and Three Dimensions. *Trends Chem.* **2019**, *1*, 172–184.

8. Geng, K.; He, T.; Liu, R.; Tan, K. T.; Li, Z.; Tao, S.; Gong, Y.; Jiang, Q.; Jiang, D. Covalent Organic Frameworks: Design, Synthesis, and Functions. *Chem. Rev.* **2020**, *120*, 8814–8933.

9. Wu, X.; Han, X.; Xu, Q.; Liu, Y.; Yuan, C.; Yang, S.; Liu, Y.; Jiang, J.; Yong, C. Chiral BINOL-Based Covalent Organic Frameworks for Enantioselective Sensing. *J. Am. Chem. Soc.* **2019**, *141*, 7081–7089.

10. Wei, Y.-S.; Zhang, M.; Zou, R.; Qiang, X. Metal–Organic Framework-Based Catalysts with Single Metal Sites. *Chem. Rev.* **2020**, *120*, 12089–12174.

11. Feng, L.; Wang, K.-Y.; Day, G. S.; Ryder, M. R.; Zhou, H.-C. Destruction of Metal–Organic Frameworks: Positive and Negative Aspects of Stability and Lability. *Chem. Rev.* **2020**, *120*, 13087–13133.

12. Huang, H.; Shen, K.; Chen, F.; Li, Y. Metal-Organic-Frameworks as a Good Platform for the Fabrication of Single-Atom Catalysts. *ACS Catal.* **2020**, *10*, 6579–6586.

13. Karmakar, A.; Illathvalappil, R.; Anothumakkool, B.; Sen, A.; Samanta, P.; Desai, A. V.; Ghosh, S. K. Hydrogen-Bonded Organic Frameworks (HOFs): A New Class of Porous Crystalline Proton-Conducting Materials. *Angew. Chem. Int. Ed.* **2016**, *55*, 10667–10671.

14. Adachi, T.; Ward, M. D. Versatile and Resilient Hydrogen-Bonded Host Frameworks. *Acc. Chem. Res.* **2016**, *49*, 2669–2679.

15. Fournier, J.-H.; Maris, T.; Wuest, J. D. Molecular Tectonics. Porous Hydrogen-Bonded Networks Built from Derivatives of 9,9'-Spirobifluorene. *J. Org. Chem.* **2004**, *69*, 1762–1775.

16. Hu, F.; Liu, C.; Wu, M.; Pang, J.; Jiang, F.; Yuan, D.; Hong, M. An Ultrastable and Easily Regenerated Hydrogen-Bonded Organic Molecular Framework with Permanent Porosity. *Angew. Chem. Int. Ed.* **2017**, *56*, 2101–2104.

17. Yin, Q.; Zhao, P.; Sa, R.-J.; Chen, G.-C.; Lu, J.; Liu, T.-F.; Cao, R. An Ultra-Robust and Crystalline Redeemable Hydrogen-Bonded Organic Framework for Synergistic Chemo-Photodynamic Therapy. *Angew. Chem. Int. Ed.* **2018**, *57*, 7691–7696.

18. Boer, S. A.; Morshedi, M.; Tarzia, A.; Doonan, C. J.; White, N. G. Supramolecular anion recognition in water: synthesis of hydrogen-bonded supramolecular frameworks. *Chem. Eur. J.* **2019**, *25*, 10006–10012.

19. Xing, G.; Yan, T.; Das, S.; Ben, T.; Qiu, S. Synthesis of Crystalline Porous Organic Salts with High Proton Conductivity. *Angew. Chem. Int. Ed.* **2018**, *57*, 5345–5349.

20. Zhou, Y.; Kan, L.; Eubank, J. F.; Li, G.; Zhang, L.; Liu, Y. Self-assembly of two robust 3D supramolecular organic frameworks from a geometrically non-planar molecule for high gas selectivity performance. *Chem. Sci.* **2019**, *10*, 6565–6571.

21. Wang, H.; Li, B.; Wu, H.; Hu, T.-L.; Yao, Z.; Zhou, W.; Xiang, S.; Chen, B. A Flexible Microporous Hydrogen-Bonded Organic Framework for Gas Sorption and Separation. *J. Am. Chem. Soc.* **2015**, *137*, 9963–9970.

22. Liang, W.; Carraro, F.; Solomon, M. B.; Bell, S. G.; Amenitsch, H.; Sumby, C. J.; White, N. G.; Falcaro, P.; Doonan, C. J. Enzyme Encapsulation in a Porous Hydrogen-Bonded Organic Framework. *J. Am. Chem. Soc.* **2019**, *141*, 14298–14305.

23. Gong, W.; Chu, D.; Jiang, H.; Chan, X.; Cui, Y.; Liu, Y. Permanent porous hydrogen-bonded frameworks with two types of Bronsted acid sites for heterogeneous asymmetric catalysis. *Nat. Commun.* **2019**, *10*, article number 600.

24. Yu, S.; Xing, G.-L.; Chen, L.-H.; Ben, T.; Su, B.-L. Crystalline Porous Organic Salts: From Micropore to Hierarchical Pores. *Adv. Mater.* **2020**, article 2003270.

25. Wang, B.; Lin, R.-B.; Zhang, Z.; Xiang, S.; Chen, B. Hydrogen-Bonded Organic Frameworks as a Tunable Platform for Functional Materials. *J. Am. Chem. Soc.* **2020**, *142*, 14399–14416.

26. Kuznetsova, S. A.; Gak, A.S.; Nelyubina, Y. V.; Larionov, V. A.; Li, H.; North, M.; Zhereb, V.P.; Smol'yakov, A.F.; Dmitrienko, A. O.; Medvedev, M.G.; Belokon, Y.N. The charge-assisted hydrogen-bonded organic framework (CAHOF) self-assembled from the conjugated acid of tetrakis(4-aminophenyl)methane and 2,6-naphthalenedisulfonate as a new class of recyclable Brønsted acid catalysts. *Beilstein J. Org. Chem.* **2020**, *16*, 1124–1134.

27. Seth, S.; Jhulki, S. Porous flexible frameworks: origins of flexibility and applications. *Mater. Horiz.* **2021**, *8*, 700–727.

28. Dolomanov, O.V.; Bourhis, L. J.; Gildea, R. J.; Howard, J. A. K.; Puschmann, H. OLEX2: a complete structure solution, refinement and analysis program. *J. Appl. Cryst.* **2009**, *42*, 339–341.

For Table of Contents Use Only

Inhibition by Water during Heterogeneous Brønsted Acid Catalysis by Three-Dimensional Crystalline Organic Salts

Alexander Gak,[1,2,3] Svetlana Kuznetsova,[1] Yulia Nelyubina,[1] Alexander A. Korlyukov,[1] Han Li,[4] Michael North,[4] Vladimir Zhereb,[5] Vlagimir Riazanov,[6] Alexander S. Peregudov,[1] Ekaterina Khakina,[1] Nikolai Lobanov,[7] Victor N. Khrustalev,[7,8] and Yuri N. Belokon[*1]

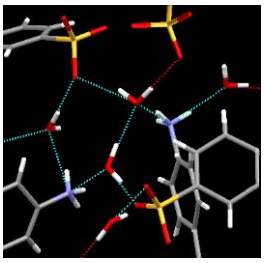

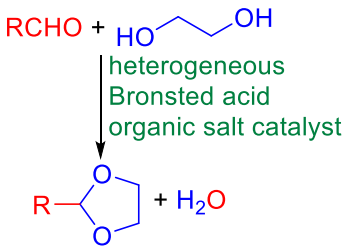

Synopsys text

Self-assembled and self-healing, metal free, recyclable, heterogeneous Brønsted acid catalysts have been developed by the protonation of aniline derivatives with aromatic sulfonic acids. The resulting three-dimensional lattices were linked by hydrogen bonds and additionally stabilized by the opposite charges of the components. They catalyzed epoxide ring-opening reactions and acetal formations.